Impaired Ca^{2+}-Dependent Activation of Large-Conductance Ca^{2+}-Activated K^+ Channels in the Coronary Artery Smooth Muscle Cells of Zucker Diabetic Fatty Rats

Tong Lu,* Dan Ye,* Tongrong He,† Xiao-li Wang,* Hai-long Wang,‡ and Hon-Chi Lee*
*Department of Internal Medicine, †Department of Anesthesiology, and ‡Department of Physiology and Biomedical Engineering, Mayo Clinic, Rochester, Minnesota 55905

ABSTRACT The large-conductance Ca^{2+}-activated K^+ (BK) channels play an important role in the regulation of cellular excitability in response to changes in intracellular metabolic state and Ca^{2+} homeostasis. In vascular smooth muscle, BK channels are key determinants of vasoreactivity and vital-organ perfusion. Vascular BK channel functions are impaired in diabetes mellitus, but the mechanisms underlying such changes have not been examined in detail. We examined and compared the activities and kinetics of BK channels in coronary arterial smooth muscle cells from Lean control and Zucker Diabetic Fatty (ZDF) rats, using single-channel recording techniques. We found that BK channels in ZDF rats have impaired Ca^{2+} sensitivity, including an increased free Ca^{2+} concentration at half-maximal effect on channel activation, a reduced steepness of Ca^{2+} dose-dependent curve, altered Ca^{2+}-dependent gating properties with decreased maximal open probability, and a shortened mean open-time and prolonged mean closed-time durations. In addition, the BK channel β-subunit-mediated activation by dehydrosoyasaponin-1 (DHS-1) was lost in cells from ZDF rats. Immunoblotting analysis confirmed a 2.1-fold decrease in BK channel β_1-subunit expression in ZDF rats, compared with that of Lean rats. These abnormalities in BK channel gating lead to an increase in the energy barrier for channel activation, and may contribute to the development of vascular dysfunction and complications in type 2 diabetes mellitus.

INTRODUCTION

The large-conductance Ca^{2+}-activated K^+ (BK) channels are allosterically regulated by intracellular free Ca^{2+} and membrane potentials (1,2). The large conductance and high density in vascular smooth muscles make these channels a key determinant in the regulation of vascular tone (3). Functional vascular BK channels are composed of pore-forming α-subunits (encoded by the *Slo* gene) and accessory β_1-subunits in a 4:4 stoichiometry (4,5). The α-subunit has seven transmembrane domains (S0–S6), including the highly conserved K^+ channel selectivity filter between S5–S6, and a voltage sensor at S4. The C-terminus has four hydrophobic segments (S7–S10) that contain a number of important regulatory sites, including two regulators of conductance for potassium (RCK1 and RCK2) (6,7) and two high-affinity Ca^{2+}-sensing regions, with Ca^{2+} concentration at half-maximal effect (EC_{50}) in the 10^{-6} M range (8,9). One is the important high-affinity Ca^{2+} sensor, Ca^{2+} bowl (892-DQDDDDDPD-900) in the RCK2 domain; the other (D362/D367) is located in the RCK1 domain (10). A recent study proposed the presence of intersubunit interfaces that connect RCK1 and RCK2 between adjacent hSlo subunits through hydrophobic interactions, and four RCK1/RCK2 dimers may form an octameric ring in a homotetrameric hSlo channel (11). There is a third Ca^{2+} sensor in the RCK/Rossman folding domain (E374 and E399) that binds Mg^{2+} and Ca^{2+} at low affinity with EC_{50} in the 10^{-3} M range (12,13). The extracellular N-terminus of the α-subunit is thought to be important for functional coupling with the β-subunit (14). Recent reports also suggested that intracellular regions of the α-subunit, including S1, S2, and S3, are required for functional and physical interaction between the BK channel α-subunits and β-subunits (15,16). Coexpression of the β_1-subunit significantly enhances the sensitivity of BK channel α-subunit to voltage-dependent and Ca^{2+}-dependent activation, and modulates channel activation, channel deactivation (17–22), and single-channel kinetics (23). The physiological importance of the β_1-subunit is demonstrated by studies with β_1-gene knockout mice, which have increased vascular tone and hypertension with uncoupling of Ca^{2+} sparks to BK channels in vascular smooth muscle cells (24,25). Despite the important physiological functions rendered by the β-subunit, the role it plays in disease states such as diabetes mellitus has not been studied in detail.

Mortality associated with cardiovascular complications in diabetes mellitus has increased by 75% in the past decade (26), contributing to more than 200,000 deaths annually in the United States (http://www.diabetes.org). The cause of vascular dysfunction in diabetes is multifactorial and includes impaired endothelial function, reduced bioavailability of endothelium-derived relaxation factors (such as nitric oxide, prostaglandin I_2, and endothelium-derived hyperpolarizing factors), and enhanced sensitivity to endothelium-derived constricting factors (27) and angiotensin II (28). In vitro vasoreactivity studies showed that diabetic vascular

Submitted May 23, 2008, and accepted for publication August 22, 2008.

Address reprint requests to Tong Lu, MD, PhD, Division of Cardiovascular Diseases, Dept. of Internal Medicine, Mayo Clinic, 200 First Street SW, Rochester, MN 55905. Tel.: 507-255-9653; Fax: 507-5386418; E-mail: lu.tong@mayo.edu.

Editor: Richard W. Aldrich.

0006-3495/08/12/5165/13 $2.00

doi: 10.1529/biophysj.108.138339

dysfunction is associated with impaired K^+ channel activities in smooth muscle cells, including those of the voltage-gated K^+ (Kv) channels (29), ATP-sensitive K^+ (K_{ATP}) channels (30–32), small-conductance Ca^{2+}-activated K^+ (SK) channels (33), and BK channels (33–37). Coronary artery smooth muscle cells cultured with high glucose showed suppressed Kv channel activation by enhanced production of hydrogen peroxide (H_2O_2) and peroxynitrite, which directly inhibit channel activity (38) and impair cAMP-dependent signaling regulation (29,39). The mechanisms that underlie BK channel dysfunction in diabetic vessels are dependent on the animal model, vessel bed, and stage of diabetes. In high-fructose diet-induced insulin-resistant rats, BK current density in mesenteric artery smooth muscle cells was reduced, but the channel Ca^{2+} sensitivity and voltage sensitivity were unchanged (37). In streptozotocin (STZ)-induced type I diabetic rats, the down-regulation of BK channel activity and decreased sensitivity to voltage-dependent activation were associated with impaired β_1-subunit function (35). During the early stages of diabetes in Zucker Diabetic Fatty (ZDF) rats, a genetically determined type 2 diabetic animal model, reduced BK channel participation in arachidonic acid-mediated coronary vasodilatation was mostly attributable to impaired biosynthesis of prostaglandin I_2 (36). In ZDF rats with more advanced diabetes, the BK channel response to Ca^{2+} and NS1619 (a BK channel α-subunit activator) activation was reduced, suggesting that the function of the α-subunit was impaired (33). Tang et al. found that the cysteine residue at 911 (C911) of hSlo, which is close to the Ca^{2+} bowl, is the major functional target of redox modulation by H_2O_2 (40). We also reported that high glucose-induced accumulation of reactive oxygen species suppressed the current density, and slowed the activation and deactivation of hSlo expressed in HEK293 cells (41). However, most of these previous studies focused on physiological regulation and on the role of BK channels in diabetic pathophysiology. The changes in biophysical properties of BK channels, such as channel kinetics and gating behaviors in diabetic vascular smooth muscle cells, have not been characterized in detail. In this study, we hypothesized that the intrinsic gating properties of vascular BK channels were altered in diabetes. Using single-channel recording techniques, we compared BK channel activities and channel protein expression in vascular smooth muscle cells from ZDF rats and age-matched Lean control rats. Our results showed profound abnormalities in the regulation of BK channels of ZDF rats. In particular, Ca^{2+}-dependent gating behaviors are substantially altered with the loss of β_1-subunit-mediated channel activation, and such changes can be explained by a significant reduction of BK channel β_1-subunit expression in ZDF rats. Finally, we employed a simple model to describe and better understand the differences in BK channel kinetics between Lean and ZDF rats. Our results may provide important insights into the fundamental mechanisms that underlie the development of vascular dysfunction and complications in diabetes.

MATERIALS AND METHODS

Animals

Male ZDF rats (Gmi-*fa*/*fa*) and age-matched Lean control rats (Gmi-*fa*/+ or +/+) were obtained from Charles River Laboratories (Wilmington, MA) at 6–8 weeks of age. All rats were housed in the Animal Care Facility of Mayo Clinic, and received a Purina 3008 modified mouse/rat diet, according to a protocol approved by the Animal Care and Use Committee of the Mayo Foundation. Blood was drawn from the tail vein, and blood glucose was monitored using an Accu-Chek glucose meter (Roche Diagnostics Co., Indianapolis, IN). Rats with blood glucose levels consistently higher than 300 mg/dL were considered diabetic. The ZDF rats 4–6 months after the development of hyperglycemia and age-matched Lean control rats were sacrificed for the experiments.

Isolation of coronary arterial smooth muscle cells

Coronary artery smooth muscle cells were dissociated enzymatically, as previously reported (42). Briefly, rat hearts were rapidly excised and placed in cold (4°C) physiological saline solution that contained 145.0 mM NaCl, 4.0 mM KCl, 0.05 mM $CaCl_2$, 1.0 mM $MgCl_2$, 10.0 mM HEPES, and 10.0 mM glucose (pH 7.2). The septal, right, and left anterior descending coronary arteries were carefully dissected free of surrounding myocardium and connective tissue, and placed in 1 mL physiological saline solution containing bovine serum albumin (0.1%, w/v) for a 10-min incubation at 37°C in a shaking water bath. The vessels were treated with 1.75 mg papain and 1.25 mg dithiothreitol in 1.0 mL saline solution for 10 min, and further digested with 1.25 mg collagenase and 1.25 mg trypsin inhibitor in 1.0 mL saline solution at 37°C for 10 min. The vessels were then washed three times with 1.0-mL aliquots of saline solution, and gently triturated with a fire-polished glass pipette until cells were completely dissociated.

Inside-out single-channel recordings

Single BK currents from coronary artery smooth muscle cells were recorded in the inside-out configuration, using an Axopatch 200B integrating amplifier and pCLAMP 8.2 software (Axon Instruments, Foster City, CA). The output signals were filtered with an eight-pole Bessel filter (902 LPF, Frequency Devices, Inc., Haverhill, MA) at 5 kHz, and digitized at 20 kHz. Patch pipettes had a typical tip resistance of 5–10 MΩ when filled with the pipette solution, which contained 140.0 mM KCl, 1.0 mM $CaCl_2$, 1.0 mM $MgCl_2$, 10.0 mM HEPES, and 1.0 mM EGTA (pH 7.4 with KOH). The bath solution contained 140.0 mM KCl, 1.0 mM $MgCl_2$, 1.0 mM EGTA, and 10.0 mM HEPES (pH 7.35 with KOH). Various amounts of Ca^{2+} were added in the bath solution to obtain the desired free Ca^{2+} concentrations (from 10^{-9} to 10^{-4} M), calculated using Chelator software, as previously described (43). The number of channels in the excised patch was determined at +60 mV in the presence of 100 μM free Ca^{2+}, a condition that was shown to activate BK channel openings maximally in rat coronary artery smooth muscle cells (43). The BK channels were identified by their unitary conductance, voltage-sensitivity, and Ca^{2+}-sensitivity. Open probability (p_O) in patches with multiple channels was determined using Fetchan in pClamp 8.2, based on the equation:

$$p_O = \left(\sum_{j=1}^{n} t_j j \right) / TN,$$

where T is the duration of recording, t_j is the time spent with $j = 1,2,3, \ldots n$ channel openings, and N is the maximal number of channel openings observed when p_O was high.

Because FETCHAN, the single-channel analysis program in pCLAMP 8.2, only allows a maximum presence of five channels for analysis, excised patches containing five or fewer channels were used for all p_O measurements.

Single-channel kinetic analysis

Excised patches containing only a single channel were used for kinetics analysis. The digital current signals were filtered at a bandwidth of 2.0 kHz with a digital Gaussian filter, and events were detected by the half-amplitude threshold criterion, using TAC software (Bruxton, Inc., Seattle, WA) with a dead time of 90 μs. The effects of the Gaussian filter on channel dwell-time durations at 50% threshold were corrected by cubic spline interpolation of the digital signal, as previously described (44). The events of subconductance opening were excluded for kinetics analysis. Dwell-time histograms were fitted with the sums of exponential probability density functions, using the TACFit program. The number of exponential components was determined by the maximal likelihood ratio test, and additional exponential components were included only when the $p > 0.95$. In the TACFit program, burst resolution was given by the burst opening that is defined by intraburst gaps shorter than the critical closed time (t_{crit}), calculated as 1.0 ms in our recording system, using the following equation (44):

$$(\alpha_f/\tau_f) \times \exp(-t_{crit}/\tau_f) = (\alpha_s/\tau_s) \times \exp(-t_{crit}/\tau_s),$$

where τ_f and α_f represent the fast time constant and its relative weight, respectively, and τ_s and α_s represent the slow time constant and its relative weight, respectively.

Single-channel kinetics analysis was performed on results obtained over a range of intracellular Ca^{2+} concentrations, using MIL software (QuB Suite, State University of New York at Buffalo, Buffalo, NY) that employs logarithm likelihood ratio tests, corrects the missed events, and gives error estimates of the fitted parameters (45,46).

The Ca^{2+}-dependent channel activation was fitted using the Hill equation (43):

$$p_{O,max} = 1/\{1 + ([Ca^{2+}]/EC_{50})^{nH}\},$$

where $p_{O,max}$ is the maximal channel open probability, $[Ca^{2+}]$ represents the intracellular free Ca^{2+} concentration, EC_{50} is the concentration at half-maximal effect, and nH is the Hill coefficient.

The p_O − voltage (V) relationships were characterized by the Boltzmann equation (43):

$$p_O = p_{O,max}/\{1 + \exp[ze\,(V_{1/2} - V)\,F/RT]\},$$

where $V_{1/2}$ is the voltage at which p_O is half of $p_{O,max}$, V is the membrane potential, z is the number of equivalent charge movements, e is the elementary charge, F is the Faraday constant, R is the universal gas constant, and T is the absolute temperature.

The change in free energy of Ca^{2+}-binding contributions to channel activation was calculated using the equation $\Delta\Delta Ca = -\Delta(zeV_{1/2})$, based on the $p_O - V$ curve shift in response to changes of the free Ca^{2+} concentrations (13). Curve fittings were performed using Igor 6.01 software (WaveMetrics, Inc., Lake Oswego, OR).

Western-blot analysis

Western blots were performed as previously described (36). Isolated aortas from three pairs of Lean and ZDF rats were homogenized, electrophoresed, transferred to nitrocellulose membrane, and immunoblotted against rabbit anti-human BK channel antibodies (1:200, custom-made) and rat anti-sloβ_1 antibodies (1:200, Alomona Labs, Jerusalem, Israel). Blots were also probed with anti-β-actin antibodies (1:500, Santa Cruz, CA) as loading controls. After extensive washing, horseradish peroxidase-conjugated secondary antibodies were added. Signals were developed using an Immun-Star HRP Chemiluminescent Kit (Bio-Rad, Hercules, CA). Optical density of the bands was analyzed using Scion Image software (Scion, Frederick, MD). Protein expression was expressed as relative abundance normalized to β-actin.

Chemicals

Dehydrosoyasaponin-1 (DHS-1) was a gift from Merck Research Laboratories (Merck & Co., Inc., Rahway, NJ). All other chemicals were purchased from Sigma-Aldrich Co. (St. Louis, MO).

Statistical analysis

Data are presented as mean ± SE. Student's t-test was used to compare data between two groups. A paired t-test was used to compare data before and after treatment. A statistically significant difference was defined as $p < 0.05$.

RESULTS

Development of hyperglycemia in ZDF rats

Blood glucose in ZDF rats started to increase after 8 weeks of age. At the time of the experiment, the Lean and ZDF rats were 27.3 ± 5.7 weeks of age ($n = 14$) and 29.8 ± 1.8 weeks of age ($n = 14$, vs. Lean rats, p = NS), respectively. The ZDF rats had markedly elevated blood glucose (544.8 ± 19.1 mg/dL vs. 179.2 ± 10.1 mg/dL in Lean rats, $n = 14$, $p < 0.05$), but body weights were not significantly different from Lean rats (429.6 ± 5.7 g in Lean rats vs. 395.8 ± 21.2 g in ZDF rats, $n = 14$ for both, p = NS), similar to previous reports (33).

Impaired Ca^{2+}-dependent BK channel activation in coronary artery smooth muscle cells in ZDF rats

We examined the Ca^{2+}-sensitivity of BK channels in Lean and ZDF rats. Fig. 1 *A* shows Ca^{2+}-dependent BK channel activities elicited at +60 mV from coronary artery smooth muscle cells of Lean and ZDF rats in the presence of various free Ca^{2+} concentrations. There was no spontaneous channel opening when the membrane was excised into a bath solution that contained 0.01 μM free Ca^{2+}. The BK channel activities in both Lean and ZDF rats became more robust with an increase of free Ca^{2+} in a dose-dependent manner. The BK channel p_O between Lean and ZDF rats became significantly different at Ca^{2+} concentrations higher than 0.5 μM. In Lean rats, p_O was 0.54 ± 0.08 at 1 μM ($n = 9$), 0.76 ± 0.07 at 10 μM ($n = 9$), and 0.78 ± 0.05 at 100 μM Ca^{2+} ($n = 9$), and p_O was significantly reduced in ZDF rats to 0.27 ± 0.07 at 1 μM ($n = 11$, $p < 0.05$ vs. Lean), 0.58 ± 0.06 at 10 μM ($n = 11$, $p < 0.05$ vs. Lean), and 0.63 ± 0.04 at 100 μM Ca^{2+} ($n = 11$, $p < 0.05$ vs. Lean). The Ca^{2+} dose-dependent curve was fitted with an EC_{50} of 1.03 ± 0.16 μM in Lean control rats ($n = 9$) and 2.44 ± 0.48 μM in ZDF rats ($n = 11$ vs. Lean, $p < 0.05$). Hence, the BK channel $p_O - Ca^{2+}$ relationship shifted rightward and downward in ZDF rats (Fig. 1 *B*). Most importantly, nH was reduced from 4.1 in Lean rats to 1.1 in ZDF rats, indicating that cooperativity of Ca^{2+}-dependent channel activation was absent in ZDF rats.

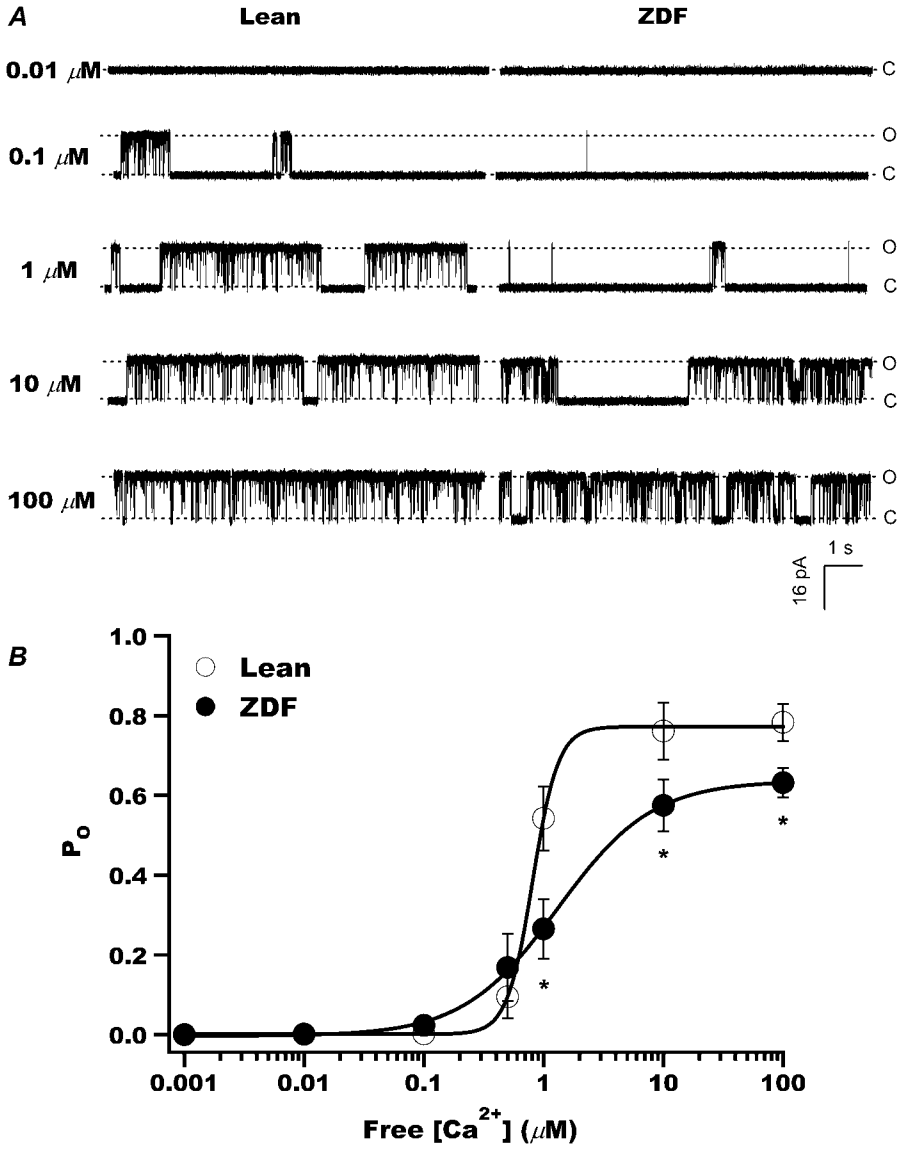

FIGURE 1 BK channels of coronary artery smooth muscle cells in ZDF rats have reduced Ca^{2+} sensitivity. (*A*) Representative inside-out single BK channel currents were recorded at +60 mV from Lean rats (*left column*) and ZDF rats (*right column*) in the presence of various free Ca^{2+} concentrations (0.01 μM to 100 μM). BK currents were activated by an increase in free Ca^{2+} concentration in both Lean and ZDF rats. (*B*) $p_O - [Ca^{2+}]$ relationships in Lean ($n = 9$) and ZDF ($n = 11$) rats were fitted using the Hill equation. There was a significant reduction in p_O in ZDF rats at Ca^{2+} concentrations ≥ 1 μM. Data are presented as mean ± SE. $^*p < 0.05$ vs. Lean. Here and in subsequent figures, C and O represent closed and open states of the BK channel, respectively.

Decreased free energy of Ca^{2+}-dependent channel activation in coronary smooth muscle cells in ZDF rats

Fig. 2 *A* shows representative BK channel tracings of Lean and ZDF rats recorded at different membrane potentials in the presence of 1 μM free Ca^{2+}. The BK channel activity increased with membrane potential depolarization in Lean and ZDF rats, both of which had the same unitary current amplitudes at the same given voltage. No spontaneous BK channel opening was discernible at −60 mV in either Lean or ZDF rats. Occasional channel openings began to appear at −20 mV in Lean rats and at +20 mV in ZDF rats (Fig. 2 *A*, *left column*), suggesting a rightward shift in the threshold of channel voltage-dependent activation in ZDF rats. Indeed, at all tested voltages above 0 mV, channel openings were more robust in Lean rats, and there was a significant reduction in channel p_O in ZDF rats over the full range of voltages, from +20 mV (0.06 ± 0.03 in ZDF rats, $n = 13$, vs. 0.31 ± 0.09 in Lean rats, $n = 15$, $p < 0.05$) to +120 mV (0.59 ± 0.06 in ZDF rats, $n = 15$, vs. 0.71 ± 0.06 in Lean rats, $n = 13$, $p < 0.05$). Fig. 2 *B* shows the BK channel $p_O - V$ relationships of Lean and ZDF rats in the absence of free Ca^{2+}, and there was a reduced maximal p_O in ZDF rats, measured at voltages higher than 150 mV (0.48 ± 0.06 in Lean rats vs. 0.20 ± 0.07 in ZDF rats, $p < 0.05$, $n = 5$ for both). There was no significant difference between Lean and ZDF rats in the voltage at half-maximal activation ($V_{1/2}$) (144.9 ± 8.8 mV in Lean rats, $n = 5$, and 132.6 ±10.8 mV in ZDF rats, $n = 5$, $p =$ NS) or in the equivalent charge movement z (0.8 e in Lean rats and 0.7 e in ZDF rats). In the presence of 1 μM Ca^{2+}, $V_{1/2}$ was 41.3 ± 4.5 mV ($n = 13$) in Lean rats, and $V_{1/2}$ shifted to the right in ZDF rats, at 89.6 ± 6.5 mV ($n = 15$, $p < 0.05$ vs. Lean rats), whereas z was unchanged, at 1.0 e in Lean rats and

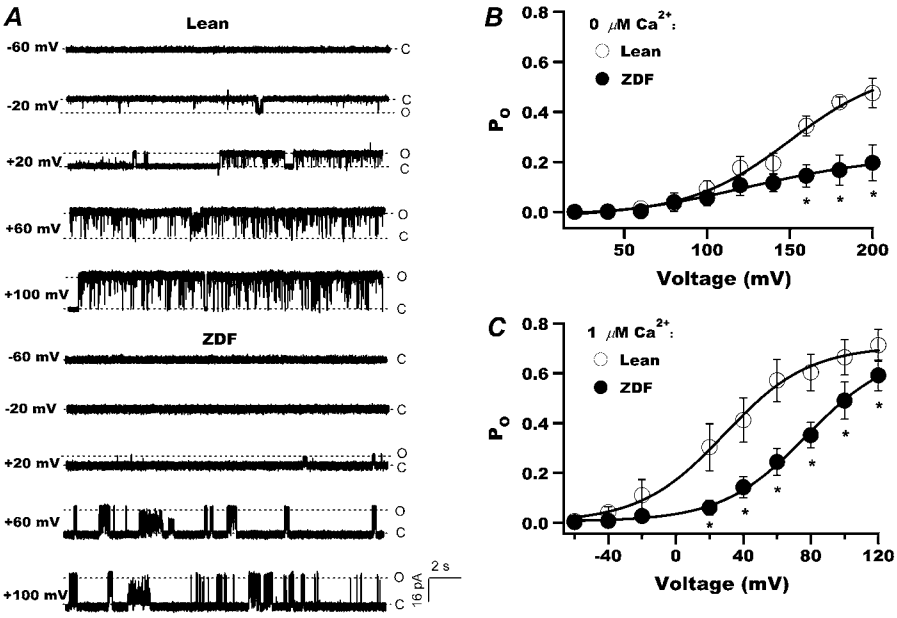

FIGURE 2 BK channels in ZDF rats have reduced response to voltage activation. (*A*) Representative tracings of single BK channel activities recorded in presence of 1 μM free Ca^{2+} at various voltages (from −60 mV to +100 mV). Channel activity was enhanced by membrane depolarization, with an activation threshold of −20 mV in Lean rats (*left column*) and +20 mV in ZDF rats (*right column*). (*B*) The $p_O - V$ relationships in Lean ($n = 15$) and ZDF ($n = 13$) rats in the absence of Ca^{2+}. The p_O was significantly lower in ZDF rats at voltages higher than +150 mV. (*C*) The $p_O - V$ relationships in Lean ($n = 15$) and ZDF ($n = 13$) rats in the presence of 1 μM Ca^{2+}. The p_O was significantly lower in ZDF rats at voltages between +20 and +120 mV, with a rightward and downward shift of the $p_O - V$ curve. Data are presented as mean ± SE. $^*p < 0.05$ vs. Lean.

1.1 *e* in ZDF rats (Fig. 2 *C*). Thus, the change in the intrinsic free energy of Ca^{2+}-binding that contributes to channel activation can be estimated, based on the shift of $p_O - V$ relationships between Lean and ZDF rats: $\Delta\Delta_{Ca} = -\Delta(zeV_{1/2})$ (13). The $\Delta\Delta_{Ca}$ was -41.4 ± 6.7 ($n = 5$) kJ/mol in Lean rats, but was reduced by 62.3% to -25.8 ± 8.7 ($n = 5, p < 0.05$) in ZDF rats, when free Ca^{2+} was increased from 0 μM to 1 μM, suggesting that Ca^{2+}-dependent activation of BK channels is less favorable in ZDF rats compared with Lean controls.

Altered BK channel kinetics in ZDF rats

For a better understanding of altered Ca^{2+}-dependent BK channel activation in ZDF rats, we further examined the Ca^{2+}-dependent gating properties in both Lean and ZDF rats. Because BK channels of ZDF rats were almost inactive at Ca^{2+} concentrations <0.1 μM, we compared single-channel gating between Lean and ZDF rats at Ca^{2+} concentrations from 1 μM to 100 μM, with a testing potential of +60 mV. Fig. 3 *A* illustrates typical tracings of inside-out single-

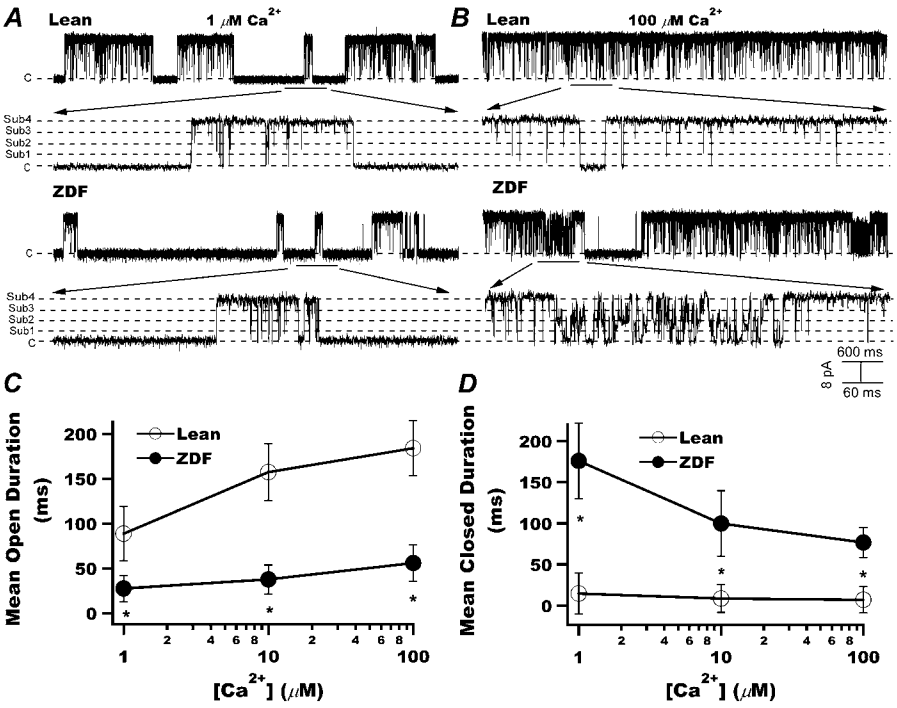

FIGURE 3 BK channels in ZDF rats have shortened mean burst durations and prolonged mean closed durations. Representative tracings of single BK currents were elicited at +60 mV in the presence of 1 μM free Ca^{2+} (*A*) and 100 μM free Ca^{2+} (*B*), in Lean (*upper tracings*) and ZDF (*lower tracings*) rats. Selected tracing segments with expanded details show longer channel-opening durations and higher p_O in Lean rats, and more frequent and stabilized subconductance levels in ZDF rats. Note that four levels of subconductance were discerned, represented by Sub1, Sub2, Sub3, and Sub4 (fully open). Plots of relationships between Ca^{2+} concentrations and mean burst durations (*C*) and mean closed times (*D*) of BK channels in Lean and ZDF rats are shown. Compared with Lean rats, ZDF rats had shorter mean burst durations and longer mean closed durations. Data are presented as mean ± SE. $^*p < 0.05$ vs. Lean ($n = 6$).

channel BK currents in Lean and ZDF rats with expanded details. In the presence of 1 μM Ca^{2+}, BK channel p_O was much higher in Lean rats than in ZDF rats. Few very brief subconductance openings were evident in both Lean and ZDF rats. An increase of Ca^{2+} to 100 μM markedly increased the channel p_O (>0.8) in both Lean and ZDF rats, but more frequent and prolonged subconductance openings were observed in ZDF rats (Fig. 3 *B*). The effects of Ca^{2+} on mean open times and on mean closed durations of BK channels in Lean and ZDF rats are illustrated in Fig. 3, *C* and *D*, respectively. Compared with Lean controls, ZDF rats had mean open times that were markedly shortened at Ca^{2+} concentrations $\geq$1 μM, and mean closed durations that were significantly prolonged at Ca^{2+} concentrations $\geq$1 μM. Because normal intracellular Ca^{2+} concentration can reach >10 μM concentrations, especially in microdomains where calcium sparks are elicited (47,48), these fundamental changes in BK channel properties are physiologically relevant. These results indicate that there is a reduction in BK channel sensitivity to activation by Ca^{2+} in ZDF rats.

Representative histograms of the BK channel probability density function in the presence of 1 μM, 10 μM, and 100 μM Ca^{2+} in Lean and ZDF rats are given in Fig. 4, *A* and *B*, respectively. For the best fit, the open dwell-time distribution histograms required at least three components: fast (τ_{O1}), intermediate (τ_{O2}), and slow (τ_{O3}) open-time constants. The closed dwell-time histograms had four components: fast (τ_{C1}), intermediate (τ_{C2}), slow (τ_{C3}), and very slow (τ_{C4}) closed-time constants. In Lean rats, an increase in Ca^{2+} concentration prolonged the open dwell times and abbreviated the closed dwell times. However, such Ca^{2+}-dependent relationships were not closely followed in ZDF rats (Table 1). For example, an increase in Ca^{2+} markedly prolonged all three open-time constants, τ_{O1}, τ_{O2}, and τ_{O3}, in Lean rats. In ZDF rats, an increase in Ca^{2+} prolonged τ_{O1} and τ_{O2}, but τ_{O3} was shortened. An increase in Ca^{2+} shortened the BK-channel closed-time constants in Lean and ZDF rats, but at any given Ca^{2+} concentration, τ_{C1}, τ_{C2}, τ_{C3}, and τ_{C4} were significantly lengthened in ZDF rats compared with Lean rats. A comparison of BK channel open-time and closed-time

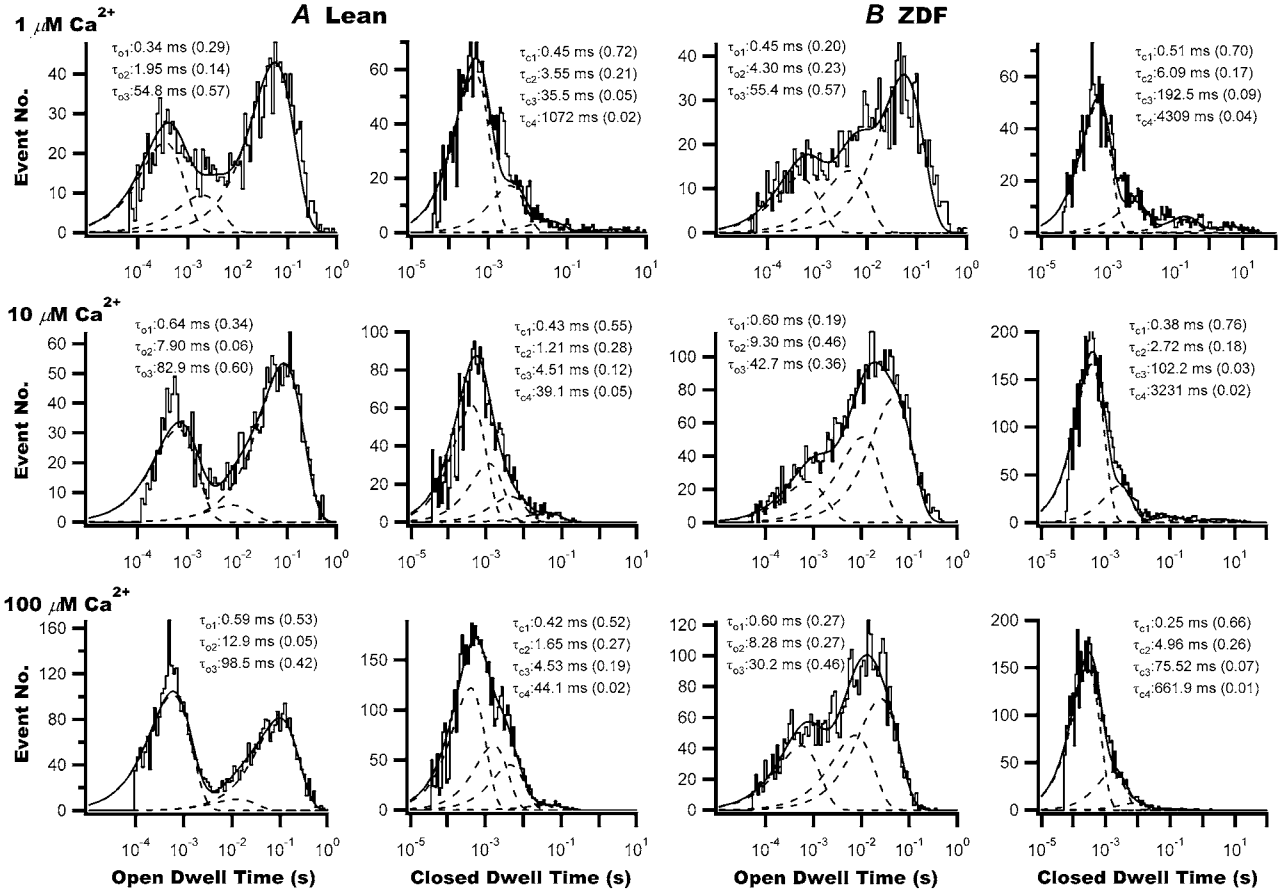

FIGURE 4 Single BK channel kinetics in Lean and ZDF rats. Representative histograms of single BK channel open and closed dwell-time durations (from one patch) in the presence of 1 μM, 10 μM, and 100 μM free Ca^{2+} in Lean rats (*A*) and ZDF rats (*B*). Data were obtained from an excised patch in inside-out configuration. Dwell-time distributions were best described by three open dwell-time components and four closed dwell-time components. An increase in cytoplasmic free Ca^{2+} from 1 μM to 100 μM prolonged all open dwell-time constants (τ_O), and shortened all closed dwell time constants (τ_C). Dashed lines represent distribution of exponential components, determined by the logarithm likelihood ratio test. The values of each time constant component and its relative weight (in parentheses) are given above each histogram.

TABLE 1 BK channel open and closed dwell-time constants and their relative weights in Lean and ZDF rats

Time constant (weight)	1 μM, Lean	1 μM, ZDF	10 μM, Lean	10 μM, ZDF	100 μM, Lean	100 μM, ZDF
τ_{O1} (ms)	0.55 ± 0.06	0.48 ± 0.06	0.85 ± 0.25	0.63 ± 0.03	0.74 ± 0.07	0.31 ± 0.19
(A_{O1})	(0.40 ± 0.07)	(0.26 ± 0.03)	(0.35 ± 0.08)	(0.47 ± 0.08)	(0.54 ± 0.05)	(0.36 ± 0.06)*
τ_{O2} (ms)	9.63 ± 1.95	4.77 ± 1.06*	10.81 ± 3.55	6.08 ± 1.28	13.92 ± 4.04	10.74 ± 4.15
(A_{O2})	(0.23 ± 0.04)	(0.41 ± 0.06)*	(0.21 ± 0.04)	(0.39 ± 0.07)*	(0.26 ± 0.06)	(0.34 ± 0.01)*
τ_{O3} (ms)	43.23 ± 9.33	39.73 ± 8.40	61.35 ± 10.70	22.47 ± 4.05*	61.97 ± 8.60	20.07 ± 3.30*
(A_{O3})	(0.38 ± 0.09)	(0.33 ± 0.07)	(0.332 ± 0.11)	(0.26 ± 0.07)	(0.22 ± 0.08)	(0.30 ± 0.09)
τ_{C1} (ms)	0.39 ± 0.06	0.61 ± 0.10	0.49 ± 0.06	0.58 ± 0.13	0.46 ± 0.06	0.54 ± 0.13
(A_{C1})	(0.61 ± 0.03)	(0.58 ± 0.09)	(0.62 ± 0.05)	(0.61 ± 0.09)	(0.61 ± 0.03)	(0.69 ± 0.09)
τ_{C2} (ms)	2.51 ± 0.472	4.26 ± 0.75	2.26 ± 0.42	4.48 ± 1.40	2.33 ± 0.61	4.74 ± 0.51*
(A_{C2})	(0.24 ± 0.03)	(0.20 ± 0.02)	(0.26 ± 0.02)	(0.27 ± 0.05)	(0.29 ± 0.01)	(0.19 ± 0.03)*
τ_{C3} (ms)	29.27 ± 10.41	198.59 ± 48.26*	29.62 ± 10.46	92.43 ± 26.17*	20.73 ± 9.78	74.02 ± 22.01
(A_{C3})	(0.03 ± 0.02)	(0.19 ± 0.07)	(0.07 ± 0.02)	(0.14 ± 0.07)	(0.11 ± 0.03)	(0.12 ± 0.08)
τ_{C4} (ms)	165.2 ± 37.74	3447.2 ± 910.9*	93.67 ± 17.38	1706.2 ± 701.6*	75.84 ± 11.88	852.18 ± 59.29*
(A_{C4})	(0.03 ± 0.02)	(0.04 ± 0.01)	(0.06 ± 0.02)	0.05 ± 0.04	(0.05 ± 0.02)	(0.09 ± 0.05)

τ_{O1}, τ_{O2}, and τ_{O3} represent fast, intermediate, and slow components of channel open dwell-time durations. τ_{c1}, τ_{c2}, τ_{c3}, and τ_{c4} represent fast, intermediate, slow, and very slow components of channel closed dwell-time durations, respectively. A_{O1-3} and A_{C1-4} represent the relative weight of each open and closed dwell-time constant, where $A_{O1} + A_{O2} + A_{O3} = 1$, and $A_{C1} + A_{C2} + A_{C3} + A_{C4} = 1$. Data are represented as mean ± SE, $n = 6$.
*$p < 0.05$ vs. Lean.

constants between Lean and ZDF rats at Ca^{2+} concentrations of 1 μM, 10 μM, and 100 μM is summarized in Table 1.

It was shown that each BK channel α-subunit has three Ca^{2+} binding sites. We demonstrate that there is a reduced *nH* for Ca^{2+}-dependent BK channel activation in ZDF rats, suggesting either a reduction in the number of Ca^{2+} binding sites or in the cooperativity of Ca^{2+} binding (Fig. 1 *B*). To describe completely all the features of BK channel Ca^{2+}-dependent and voltage-dependent activation requires a 50-state, two-tiered model (2,49). Here, we tried to use the simplest model that could describe our experimental results. Because BK channel kinetics analysis suggests the presence of at least three open states and four closed states in the range of Ca^{2+} concentrations tested, a minimal kinetic scheme could be represented by Scheme I in Fig. 5 *A* (50), where the transitions between states $C_0 \leftrightarrow C_1$, $C_1 \leftrightarrow C_2$, and $C_2 \leftrightarrow C_3$ are Ca^{2+}-dependent. Using single-channel kinetic-analysis software, we estimated the rate constants between each state transition of the BK channel in Lean and ZDF rats, and the group results from three experiments are listed in Table 2. The energy barrier for channel activation could be calculated using the equation $G = RT \ln K_{eq}$ (51), where G is the energy barrier, K_{eq} represents the equilibrium constant of the transition state, R is the universal gas constant, and T is the absolute temperature. Hence, the total energy barriers (G_T) can be determined by the sum of each energy barrier of the transition state. The relationships between G_T and the logarithm of Ca^{2+} concentrations are plotted in Fig. 5 *B* ($n = 3$ for Lean and ZDF rats, respectively). The $G_T - \log[Ca^{2+}]$ relationships can be fitted by a linear equation with a slope of 16.6 for both Lean and ZDF rats. However, the G_T for BK channel activation was increased by 8.6-fold at all given Ca^{2+} concentrations. The upward shift of the $G_T - \log[Ca^{2+}]$ relationship in ZDF rats indicates less thermodynamically favorable conditions of Ca^{2+}-dependent BK channel activation in ZDF rats, and that at any given Ca^{2+} concentration, there is a greater energy barrier to overcome for BK channel activation. We did not include the transitions between $O_1 \leftrightarrow O_2$ and $O_2 \leftrightarrow O_3$ in the model, because the loop transition model would not change the values of the total energy barrier obtained from Scheme I (Fig. 5 *A*), and would not change our conclusions.

Impaired BK channel activity with loss of β_1-subunit-mediated channel activation and reduced β_1-subunit expression in smooth muscle cells of ZDF rats

Because the BK channel β-subunit is known to regulate channel sensitivity to Ca^{2+}, we examined the function of the β_1-subunit using a specific BK channel β-subunit activator, DHS-1 (52), to determine whether β_1-subunit function contributes to the mechanism underlying impaired BK channel function in ZDF rats. Fig. 6 *A* shows representative tracings of inside-out BK currents elicited at +60 mV in the presence of 0.5 μM free Ca^{2+}, before and after exposure to 0.1 μM DHS-1, followed by a washing out of DHS-1. In Lean rats, DHS-1 significantly enhanced channel p_O from 0.21 ± 0.09 at baseline to 0.54 ± 0.08 with DHS-1 ($n = 7$, $p < 0.05$ vs. baseline), and this effect was reversible upon washing out. In contrast, DHS-1 had no significant effects on BK channel activities in ZDF rats (0.17 ± 0.06 at baseline and 0.28 ± 0.08 with DHS-1, $n = 7$, p = NS), suggesting that β_1-subunit-mediated BK channel activation was significantly reduced in

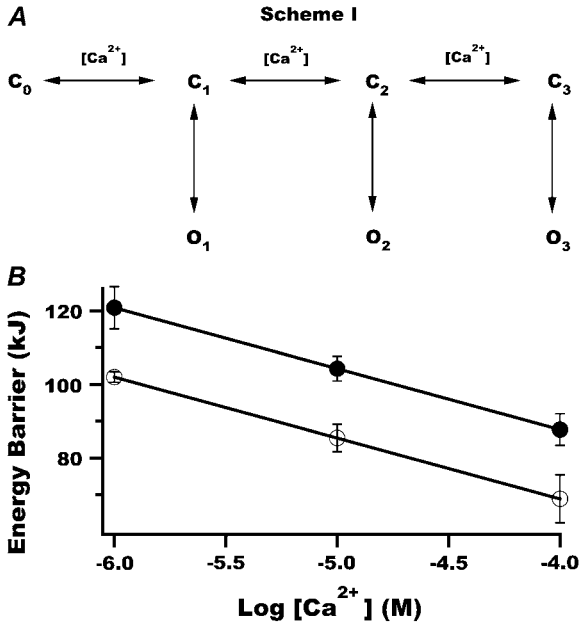

FIGURE 5 Increased energy barriers of Ca^{2+}-dependent BK channel activation in ZDF rats. (*A*) BK channel-gating can be described by a simple kinetics model, as shown in Scheme I. O and C represent the channel open states and closed states, where transitions between $C_0 \leftrightarrow C_1$, $C_1 \leftrightarrow C_2$, and $C_2 \leftrightarrow C_3$ are Ca^{2+}-dependent. (*B*) Total energy barriers (G_T) for BK channel activation, calculated from Scheme I (Fig. 5 *A*) in Lean and ZDF rats, are plotted against the logarithm of Ca^{2+} concentrations. The $G_T - \log[Ca^{2+}]$ relationship is fitted with a linear equation, with $G_T = 2.5 + 16.6 \log[Ca^{2+}]$ in Lean rats, and $G_T = 21.4 + 16.6 \log[Ca^{2+}]$ in ZDF rats. Hence, an 8.6-fold increase in energy barrier for BK-channel activation is present in ZDF rats at all given Ca^{2+} concentrations.

ZDF rats. A comparison of the DHS-1 effects between Lean and ZDF rats is summarized in the bar graphs of Fig. 6 *A*. We then determined the protein expression of BK channel α-subunits and β_1-subunits in the aortas of Lean and ZDF rats. The immunoblots of BK channel α-subunits and β_1-subunits from three pairs of Lean and ZDF rat aortas are illustrated in Fig. 6 *B*. The group results of densitometric analysis are summarized in the bar graphs. There was no significant difference in BK channel α-subunit expression between Lean and ZDF rats (0.39 ± 0.02 in Lean rats vs. 0.37 ± 0.01 in ZDF rats, $n = 3, p =$ NS). These results are similar to those reported by other laboratories (34). However, BK channel β_1-subunit expression was reduced by 2.1-fold in ZDF rats, from 0.132 ± 0.03 in Lean rats to 0.062 ± 0.01 in ZDF rats ($n = 3$, $p < 0.05$). These important results indicate that β_1-subunit expression is reduced, and that β_1-subunit-mediated regulation of BK channel function is impaired, in ZDF rats.

Increased BK channel subconductance openings in ZDF rats

It is known that BK channels exhibit multiple levels of subconductance, in which some but not all four channel subunits are in the open state and BK channel subconductance activity is thought to be regulated by the β_1-subunit (53–56). We found that BK channel subconductance openings appeared to be more frequent and stable in ZDF rats, especially in the presence of high free Ca^{2+} (≥ 10 μM). Fig. 7 *A* illustrates a typical tracing recorded at +60 mV, with expanded details showing multiple subconductance levels. The amplitude histograms were fitted with a Gaussian function, and showed four levels of conductance (three levels of subconductance), i.e., Sub1, Sub2, Sub3, and Sub4 (fully open), with unitary current amplitudes of 4 pA, 8 pA, 12 pA, and 16 pA, respectively (Fig. 7 *B*). The cooperative conformational changes of channel subunits can be estimated from the relationship between the number of subconductance states and their relative frequencies. Relative frequencies were plotted against each subconductance state in Lean and ZDF rats in Fig. 7 *C*. These relationships can be fitted by a single exponential function: $y = \omega \cdot \exp(\psi \cdot x)$, where ω is the fitting constant, and ψ is the coefficient of subunit conformational change. The coefficient of BK channel subunit conformational change was estimated to be 3.3 in Lean rats, and 1.4 in ZDF rats. These findings match our results, i.e., that the *nH* of Ca^{2+}-dependent channel activation was reduced from 4.1 in Lean rats to 1.1 in ZDF rats (Fig. 1 *B*). Hence, *nH* in the Ca^{2+}-dependent channel activation curve is in agreement with the cooperativity of subunit conformational change in tetrameric BK channels. These observations suggest that Ca^{2+} cooperativity and subunit conformational changes may be coupled, but such coupling appeared to be impaired in the BK channels of ZDF rats.

DISCUSSION

We compared the single-channel kinetics of vascular BK channels between genetically determined type II diabetic ZDF rats and aged-matched Lean control rats. We made several novel observations. First, BK channels in ZDF rats have reduced Ca^{2+} sensitivity. Second, BK channels in ZDF rats have altered Ca^{2+}-dependent gating, showing shortened open dwell times, prolonged closed dwell times, and more frequent subconductance openings. Third, BK channels in ZDF rats have a significant impairment in β_1-subunit-mediated

TABLE 2 State transition rate constants of BK channels in Lean and ZDF rats

(S^{-1})	$C_0 \rightarrow C_1$*	$C_1 \rightarrow C_0$	$C_1 \rightarrow C_2$*	$C_2 \rightarrow C_1$	$C_2 \rightarrow C_3$*	$C_3 \rightarrow C_2$	$C_1 \rightarrow O_0$	$O_1 \rightarrow C_1$	$C_2 \rightarrow O_2$	$O_2 \rightarrow C_2$	$C_3 \rightarrow O_3$	$O_3 \rightarrow C_3$
Lean	45.1 ± 23.5	5.8 ± 5.0	296 ± 239	1.0 ± 0.7	7.0 ± 6.6	218 ± 66	4.7 ± 2.9	167 ± 53	655 ± 170	202 ± 129	327 ± 138	202 ± 37.1
ZDF	0.9 ± 0.5	70.1 ± 69.7	23.2 ± 17.0	560 ± 210	0.9 ± 0.9	6.9 ± 6.8	2864 ± 526	128 ± 79	251 ± 21	2117 ± 613	17.8 ± 17.2	14.8 ± 9.4

Data are presented as mean ± SE ($n = 3$ for both groups).
*Transition is Ca^{2+}-dependent (in $\mu M\ s^{-1}$).

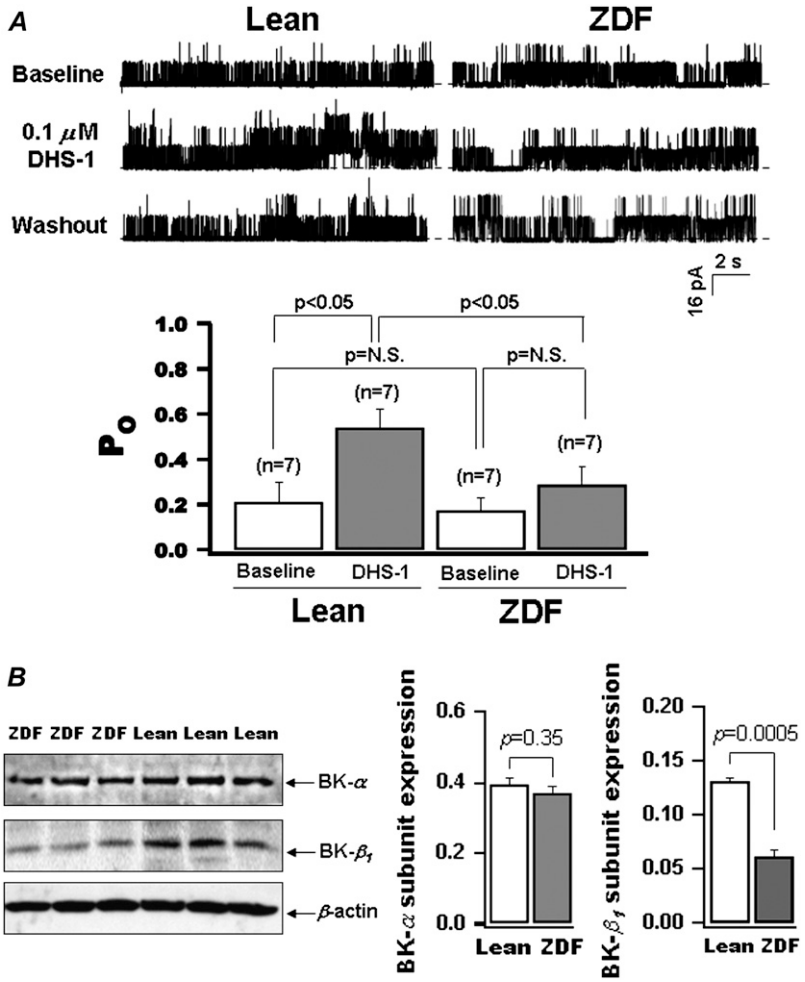

FIGURE 6 Impaired β_1-subunit-dependent activation and reduced β_1-subunit expression in BK channels of ZDF rats. (*A*) BK currents in Lean (*left*) and ZDF (*right*) rats were recorded from inside-out excised patches at +60 mV in presence of 0.5 μM free Ca^{2+} at baseline, with application of 0.1 μM DHS-1, followed by washing out. Application of DHS-1 significantly increased BK channel p_O in Lean rats, but not in ZDF rats. Comparison of DHS-1 effects on BK channel activity between Lean and ZDF rats is summarized in bar graphs. (*B*) Immunoblot analysis of BK channel α-subunit and β_1-subunit expression in aortas from three pairs of Lean and ZDF rats. Protein expression was expressed as relative abundance, normalized to β-action. There was a 2.1-fold decrease in β_1-subunit expression in aortas of ZDF rats, whereas α-subunit expression was unchanged compared with Lean rats.

activation of BK channels, associated with a substantial decrease in BK channel β_1-subunit expression but not in α-subunit expression. These alterations in the biophysical and biochemical properties of BK channels result in an increase of energy barriers for channel activation, and may contribute to diabetic vascular dysfunction.

It is well-known that the BK channel β_1-subunit is an important regulator of BK channel function. It modulates the

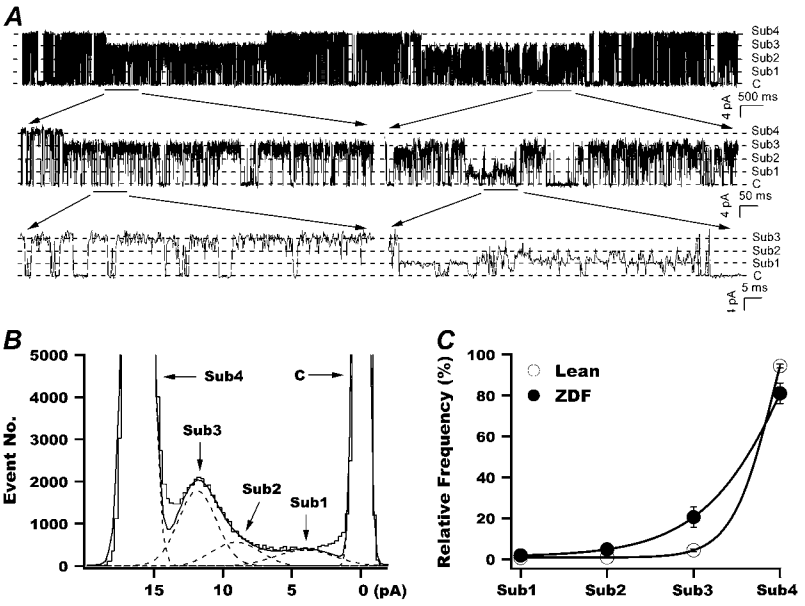

FIGURE 7 Increased BK channel subconductance openings in ZDF rats. (*A*) Representative single BK current recordings were obtained at +60 mV in the presence of 1 μM free Ca^{2+}, with selected segments that showed expanded details, demonstrating presence of four sublevels of openings. (*B*) Amplitude histogram was fitted using a Gaussian function, and showed four peaks with unitary amplitudes of 4 pA (Sub1), 8 pA (Sub2), 12 pA (Sub3), and 16 pS (Sub4 or fully open). Relative frequencies of each subconductance state were calculated by the area under each component of the Gaussian function. (*C*) Relative frequencies were plotted against subconductance states, and relationships were fitted using a single exponential function. Coefficient of subconductance conformational changes was estimated to be 3.3 in Lean rats ($n = 3$), and 1.4 in ZDF rats ($n = 3$), for a reduction of 2.3-fold in the latter.

Ca^{2+}-dependent activation and deactivation gating of whole-cell Slo currents (17–21), reduces the steepness of the Ca^{2+} response curve (21), increases the maximal p_O, prolongs the open dwell times, and abbreviates the closed dwell times in single-channel kinetics (23). However, all these experiments were performed on expressed Slo channels, and the physiological relevance of the β_1-subunit modulation of native BK channels is not clear. In this study, we provide compelling evidence that BK channels in native vascular smooth muscle cells from type II diabetic rats show altered gating behaviors that can be attributed to the deficiency of β_1-subunit functions. We found that the cooperativity of Ca^{2+}-dependent BK channel activation was lost in diabetes, as indicated by a reduction in the coefficient of subunit conformation and in the Hill coefficient. Moreover, kinetic analysis showed that BK channels in ZDF rats had a prolongation of closed dwell-time durations and a shortening of open dwell-time durations, with an increase in energy barriers for Ca^{2+}-dependent BK channel activation. However, we do not know whether reduced Ca^{2+} cooperativity occurs among Ca^{2+} sensors of the same channel α-subunit or among those of different α-subunits of the tetrameric channel. Qian et al. (57) reported that intrasubunit cooperation is more effective in mediating channel Ca^{2+} sensitivity. Impairment of intrasubunit cooperativity reduces not only the efficiency but also the efficacy of Ca^{2+}-dependent activation of hSlo, whereas impairment of intersubunit cooperativity affects only the efficiency of Ca^{2+}-dependent activation (57). Because both the efficiency and efficacy of Ca^{2+}-dependent activation were reduced in ZDF rats, it is likely that impaired intrasubunit Ca^{2+} cooperative binding is the culprit. The ZDF rats showed a rightward and downward shift in the $p_O - V$ curve, suggesting impaired voltage-dependent BK channel activation. Because the free energy of Ca^{2+}-binding for channel activation was reduced but not the equivalent charge movement z, the voltage-dependent changes in ZDF rats are likely secondary to Ca^{2+}-dependent changes in channel-gating properties.

A key finding in this study is that the function of BK channel β_1-subunits is impaired in ZDF rats. Recently, in STZ-induced type I diabetic animals, BK channel β_1-subunit mRNA transcripts were found to be reduced by 60% (35). However, using immunohistochemistry techniques, Burnham et al. reported that the expression of BK channel α-subunits and β_1-subunits in the mesenteric arteries was not significantly different between Lean and ZDF rats (33). In our experiments, we found a 2.1-fold reduction of BK channel β_1-subunit expression in the aortas of ZDF rats. The discrepancy between these studies may be attributable to the use of vessels from different tissue beds and a difference in methodologies. Although we did not directly determine β_1-subunit expression in coronary arteries, the loss of DHS-1-mediated BK channel activation in the coronary artery smooth muscle cells of ZDF rats could be directly explained by a substantial reduction in β_1-subunit expression, similar to that in the aorta. We also found that the expression of the BK channel α-subunit in Lean and ZDF rats was the same, and similar to that reported by Burham et al. (33). However, we cannot exclude the possibility that the BK channel α-subunit may be functionally impaired in ZDF rats. The α-subunit is known to be a target of high glucose-mediated oxidative modulation (41), and oxidation of SloC911 was shown to have effects comparable to those of a functional β_1-subunit knockout (40).

It requires more than a 50-state model to account completely for all the features of BK channel Ca^{2+}-dependent and voltage-dependent activation (2,49). However, we found that a simplified model (Scheme I, Fig. 5 *A*) could adequately describe the difference in Ca^{2+}-dependent gating between Lean and ZDF rats, similar to a previous report (50). Here, O_2, O_3, and O_1 represent the longest, intermediate, and shortest open states of the BK channel in Lean rats, whereas O_3, O_2, and O_1 are the longest, intermediate, and shortest open states for ZDF rats. The transition rates from C_2 to O_2 and from C_3 to O_3 are faster than those from C_1 to O_1 in Lean rats. In contrast, the transition from C_1 to O_1 is fastest in ZDF rats. These channel gating properties suggest that BK channels dwell in longer open states in Lean rats, but have more frequent flickering openings in ZDF rats. According to Scheme I (Fig. 5 *A*), the total energy barrier for channel activation at any given Ca^{2+} concentration was 8.6-fold higher in ZDF rats, suggesting that activations of BK channels in ZDF rats are thermodynamically less favorable. In the simplified model, we did not include the transitions between open states, although it was shown that a Ca^{2+}-dependent transition between $O_1 \leftrightarrow O_2$ and $O_2 \leftrightarrow O_3$ may exist. However, adding two more transitions between $O_1 \leftrightarrow O_2$ and $O_2 \leftrightarrow O_3$ would not change the total energy barrier, and we can easily calculate the apparent Ca^{2+} dissociation constants of $O_1 \leftrightarrow O_2$ and $O_2 \leftrightarrow O_3$ by applying the principle of microscopic reversibility (58) to the resulting closed cycles: O_1–C_1–C_2–O_2 and O_2–C_2–C_3–O_3. Under equilibrium conditions, the loop equilibrium constants must obey the relationship: $K_{C1-O1} \times K^*_{O1-O2} = K^*_{C1-C2} \times K_{C2-O2}$ and $K_{C2-O2} \times K^*_{O2-O3} = K_{C2-C3} \times K^*_{C3-O3}$, where K_{C1-O1}, K_{C2-O2}, and K_{C3-O3} are the opening equilibrium constants, and K^*_{O1-O2}, K^*_{C1-C2}, K^*_{O2-O3}, and K^*_{C2-C3} are apparent Ca^{2+} dissociation constants between the respective resting states (or closed states) and open states. With the values of K_{C1-O1}, K^*_{C1-C2}, K_{C2-O2}, K^*_{C2-C3}, and K_{C3-O3} from Scheme I (Fig. 5 *A*; Table 2), K^*_{O1-O2} and K^*_{O2-O3} can be calculated and shown to be 0.39 μM and 15.52 μM, respectively, in Lean rats, and 0.13 μM and 52.32 μM, respectively, in ZDF rats. The greater values of Ca^{2+} dissociation constants in ZDF rats indicate that the Ca^{2+} binding of BK channel open states was less stable in these animals, leading to a shortening of the longer open dwell-time durations, and increasing the frequency of flickering openings. It is worth emphasizing that adding two more transitions among open states in the loop transition model could only increase the probability of a logarithm likelihood ratio test, but it would not change our conclusions in Scheme I (Fig. 5 *A*).

Subconductance openings were observed in many channels, including BK channels (23,53,56), *Shaker* channels (59,60), and cystic fibrosis transmembrane conductance regulator channels (61,62). Two mechanisms for subconductance openings have been proposed. The first involves a blockage of channel subunit conduction. It was shown that dendrotoxin I inhibited BK channels and produced subconductance states by a direct interaction with the channel cytoplasmic pore (63). Coexpression of wild-type Slo channels and the tetraethylammonium (TEA)-insensitive Slo mutant channels (mSloY294V) resulted in four levels of subconductance, according to the composition (the wild-type/mSloY294V ratio) of the tetrameric channel, in recordings with TEA in the pipette solution (54,57). The second mechanism involves the individual activation of each tetrameric K^+ channel subunit. Using a chimeric Kv2.1 channel construct containing tandem dimers that linked two K^+ channel subunits with different voltage-activation thresholds, Chapman et al. found two levels of subconductance when the membrane was depolarized to potentials between the activation thresholds of the subunits (64). The authors concluded that each subunit must change its conformation from a closed state to an open state as the pore undergoes heteromeric conformations in which some subunits are in the open state, but other subunits remain closed, resulting in subconductance openings (64). Under normal conditions, transitions of heteromeric conformational states are too transient to be observed, and the sojourns could only be detected when transitions were slowed (53). The reason that ZDF BK channels undergo more subconductance openings is not understood. Like Kv channels, however, BK channels are tetrameric and allosterically activated by voltage and by intracellular free Ca^{2+}. Hence, BK channel subconductance states may also arise from subunit heteromeric pore conformational changes. Subconductance states would be more frequently discernible as transitions between subunit conformations become slower. This is in agreement with our results, i.e., that there is a higher energy barrier for Ca^{2+}-dependent channel activation in diabetic BK channels. It was suggested that the functional coupling between α-subunits and β_1-subunits is a key determinant of BK channel subconductance openings (23). Loss of β_1-subunit function would cause impaired channel sensitivity to voltage and intracellular Ca^{2+} (17–22). Hence, reduced BK channel β_1-subunit expression in ZDF rats would favor BK channel subconductance openings. In addition, impaired allosteric transitions between the fully open and fully closed states of BK channels in ZDF rats may contribute to the increase in subconductance openings (55).

To the best of our knowledge, we have presented the first compelling evidence of a physical and functional loss of β_1-subunits in native vascular BK channels in ZDF rats. These changes may account for the profound abnormalities in channel gating properties, including Ca^{2+}-dependent activation. Results from this study have important physiological and clinical implications, and may help us better understand the mechanisms that underlie diabetic vascular BK channel dysfunction, and moreover may provide novel insights into the development of approaches for the management of diabetic vasculopathy.

We thank Dr. Steven M. Sine for helpful critique of the manuscript. The DHS-1 was kindly provided by Merck & Co.

T.L. is the recipient of a Junior Faculty Award from the American Diabetes Association. This work was supported by grants from the National Institutes of Health (HL-74180 and HL-080118 to H.L.).

REFERENCES

1. Cox, D. H., J. Cui, and R. W. Aldrich. 1997. Allosteric gating of a large conductance Ca-activated K^+ channel. *J. Gen. Physiol.* 110:257–281.
2. Rothberg, B. S., and K. L. Magleby. 2000. Voltage and Ca^{2+} activation of single large-conductance Ca2+-activated K^+ channels described by a two-tiered allosteric gating mechanism. *J. Gen. Physiol.* 116:75–99.
3. Tanaka, Y., K. Koike, and L. Toro. 2004. MaxiK channel roles in blood vessel relaxations induced by endothelium-derived relaxing factors and their molecular mechanisms. *J. Smooth Muscle Res.* 40:125–153.
4. Knaus, H. G., M. Garcia-Calvo, G. J. Kaczorowski, and M. L. Garcia. 1994. Subunit composition of the high conductance calcium-activated potassium channel from smooth muscle, a representative of the mSlo and slowpoke family of potassium channels. *J. Biol. Chem.* 269:3921–3924.
5. Jiang, Z., M. Wallner, P. Meera, and L. Toro. 1999. Human and rodent MaxiK channel β-subunit genes: cloning and characterization. *Genomics.* 55:57–67.
6. Jiang, Y., A. Pico, M. Cadene, B. T. Chait, and R. MacKinnon. 2001. Structure of the RCK domain from the *E. coli* K^+ channel and demonstration of its presence in the human BK channel. *Neuron.* 29:593–601.
7. Jiang, Y., A. Lee, J. Chen, M. Cadene, B. T. Chait, and R. MacKinnon. 2002. Crystal structure and mechanism of a calcium-gated potassium channel. *Nature.* 417:515–522.
8. Schreiber, M., A. Yuan, and L. Salkoff. 1999. Transplantable sites confer calcium sensitivity to BK channels. *Nat. Neurosci.* 2:416–421.
9. Xia, X. M., X. Zeng, and C. J. Lingle. 2002. Multiple regulatory sites in large-conductance calcium-activated potassium channels. *Nature.* 418:880–884.
10. Zeng, X. H., X. M. Xia, and C. J. Lingle. 2005. Divalent cation sensitivity of BK channel activation supports the existence of three distinct binding sites. *J. Gen. Physiol.* 125:273–286.
11. Yusifov, T., N. Savalli, C. S. Gandhi, M. Ottolia, and R. Olcese. 2008. The RCK2 domain of the human BKCa channel is a calcium sensor. *Proc. Natl. Acad. Sci. USA.* 105:376–381.
12. Zhang, X., C. R. Solaro, and C. J. Lingle. 2001. Allosteric regulation of BK channel gating by Ca^{2+} and Mg^{2+} through a nonselective, low affinity divalent cation site. *J. Gen. Physiol.* 118:607–636.
13. Shi, J., G. Krishnamoorthy, Y. Yang, L. Hu, N. Chaturvedi, D. Harilal, J. Qin, and J. Cui. 2002. Mechanism of magnesium activation of calcium-activated potassium channels. *Nature.* 418:876–880.
14. Meera, P., M. Wallner, M. Song, and L. Toro. 1997. Large conductance voltage- and calcium-dependent K^+ channel, a distinct member of voltage-dependent ion channels with seven N-terminal transmembrane segments (S0–S6), an extracellular N terminus, and an intracellular (S9–S10) C terminus. *Proc. Natl. Acad. Sci. USA.* 94:14066–14071.
15. Morrow, J. P., S. I. Zakharov, G. Liu, L. Yang, A. J. Sok, and S. O. Marx. 2006. Defining the BK channel domains required for β1-subunit modulation. *Proc. Natl. Acad. Sci. USA.* 103:5096–5101.

16. Orio, P., Y. Torres, P. Rojas, I. Carvacho, M. L. Garcia, L. Toro, M. A. Valverde, and R. Latorre. 2006. Structural determinants for functional coupling between the β and α subunits in the Ca^{2+}-activated K^+ (BK) channel. *J. Gen. Physiol.* 127:191–204.

17. McManus, O. B., L. M. Helms, L. Pallanck, B. Ganetzky, R. Swanson, and R. J. Leonard. 1995. Functional role of the β subunit of high conductance calcium-activated potassium channels. *Neuron.* 14:645–650.

18. Meera, P., M. Wallner, Z. Jiang, and L. Toro. 1996. A calcium switch for the functional coupling between α (hslo) and β subunits (Kv,caβ) of maxi K channels. *FEBS Lett.* 385:127–128.

19. Tanaka, Y., P. Meera, M. Song, H. G. Knaus, and L. Toro. 1997. Molecular constituents of maxi KCa channels in human coronary smooth muscle: predominant α + β subunit complexes. *J. Physiol. (Lond.)* 502:545–557.

20. Xia, X. M., J. P. Ding, and C. J. Lingle. 1999. Molecular basis for the inactivation of Ca^{2+}- and voltage-dependent BK channels in adrenal chromaffin cells and rat insulinoma tumor cells. *J. Neurosci.* 19:5255–5264.

21. Cox, D. H., and R. W. Aldrich. 2000. Role of the β1 subunit in large-conductance Ca^{2+}-activated K^+ channel gating energetics. Mechanisms of enhanced Ca^{2+} sensitivity. *J. Gen. Physiol.* 116:411–432.

22. Giangiacomo, K. M., A. Kamassah, G. Harris, and O. B. McManus. 1998. Mechanism of maxi-K channel activation by dehydrosoyasaponin-I. *J. Gen. Physiol.* 112:485–501.

23. Nimigean, C. M., and K. L. Magleby. 1999. The β subunit increases the Ca^{2+} sensitivity of large conductance Ca^{2+}-activated potassium channels by retaining the gating in the bursting states. *J. Gen. Physiol.* 113:425–440.

24. Brenner, R., G. J. Perez, A. D. Bonev, D. M. Eckman, J. C. Kosek, S. W. Wiler, A. J. Patterson, M. T. Nelson, and R. W. Aldrich. 2000. Vasoregulation by the β1 subunit of the calcium-activated potassium channel. *Nature.* 407:870–876.

25. Pluger, S., J. Faulhaber, M. Furstenau, M. Lohn, R. Waldschutz, M. Gollasch, H. Haller, F. C. Luft, H. Ehmke, and O. Pongs. 2000. Mice with disrupted BK channel β1 subunit gene feature abnormal Ca^{2+}- spark/STOC coupling and elevated blood pressure. *Circ. Res.* 87:E53–E60.

26. Luscher, T. F., M. A. Creager, J. A. Beckman, and F. Cosentino. 2003. Diabetes and vascular disease: pathophysiology, clinical consequences, and medical therapy: part II. *Circulation.* 108:1655–1661.

27. De Vriese, A. S., T. J. Verbeuren, J. Van de Voorde, N. H. Lameire, and P. M. Vanhoutte. 2000. Endothelial dysfunction in diabetes. *Br. J. Pharmacol.* 130:963–974.

28. Deinum, J., and N. Chaturvedi. 2002. The renin-angiotensin system and vascular disease in diabetes. *Semin. Vasc. Med.* 2:149–156.

29. Bubolz, A. H., H. Li, Q. Wu, and Y. Liu. 2005. Enhanced oxidative stress impairs cAMP-mediated dilation by reducing Kv channel function in small coronary arteries of diabetic rats. *Am. J. Physiol. Heart Circ. Physiol.* 289:H1873–H1880.

30. Kersten, J. R., L. A. Brooks, and K. C. Dellsperger. 1995. Impaired microvascular response to graded coronary occlusion in diabetic and hyperglycemic dogs. *Am. J. Physiol. Heart Circ. Physiol.* 268:H1667–H1674.

31. Bouchard, J. F., E. C. Dumont, and D. Lamontagne. 1999. Modification of vasodilator response in streptozotocin-induced diabetic rat. *Can. J. Physiol. Pharmacol.* 77:980–985.

32. Miura, H., R. E. Wachtel, F. R. Loberiza, Jr., T. Saito, M. Miura, A. C. Nicolosi, and D. D. Gutterman. 2003. Diabetes mellitus impairs vasodilation to hypoxia in human coronary arterioles: reduced activity of ATP-sensitive potassium channels. *Circ. Res.* 92:151–158.

33. Burnham, M. P., I. T. Johnson, and A. H. Weston. 2006. Reduced Ca^{2+}-dependent activation of large-conductance Ca^{2+}-activated K^+ channels from arteries of type 2 diabetic Zucker Diabetic Fatty rats. *Am. J. Physiol. Heart Circ. Physiol.* 290:H1520–H1527.

34. Zhou, W., X. L. Wang, T. L. Kaduce, A. A. Spector, and H. C. Lee. 2005. Impaired arachidonic acid-mediated dilation of small mesenteric Arteries in Zucker Diabetic Fatty Rats. Am. J. Physiol. Heart. Circ. Physiol. 288:H2210–H2218.

35. McGahon, M. K., D. P. Dash, A. Arora, N. Wall, J. Dawicki, D. A. Simpson, C. N. Scholfield, J. G. McGeown, and T. M. Curtis. 2007. Diabetes downregulates large-conductance Ca^{2+}-activated potassium β 1 channel subunit in retinal arteriolar smooth muscle. *Circ. Res.* 100: 703–711.

36. Lu, T., X. L. Wang, T. He, W. Zhou, T. L. Kaduce, Z. S. Katusic, A. A. Spector, and H. C. Lee. 2005. Impaired arachidonic acid-mediated activation of large-conductance Ca^{2+}-activated K^+ channels in coronary arterial smooth muscle cells in Zucker Diabetic Fatty rats. *Diabetes.* 54:2155–2163.

37. Dimitropoulou, C., G. Han, A. W. Miller, M. Molero, L. C. Fuchs, R. E. White, and G. O. Carrier. 2002. Potassium (BK(Ca)) currents are reduced in microvascular smooth muscle cells from insulin-resistant rats. *Am. J. Physiol. Heart Circ. Physiol.* 282:H908–H917.

38. Liu, Y., K. Terata, Q. Chai, H. Li, L. H. Kleinman, and D. D. Gutterman. 2002. Peroxynitrite inhibits Ca^{2+}-activated K^+ channel activity in smooth muscle of human coronary arterioles. *Circ. Res.* 91:1070–1076.

39. Li, H., Q. Chai, D. D. Gutterman, and Y. Liu. 2003. Elevated glucose impairs cAMP-mediated dilation by reducing Kv channel activity in rat small coronary smooth muscle cells. *Am. J. Physiol. Heart Circ. Physiol.* 285:H1213–H1219.

40. Tang, X. D., M. L. Garcia, S. H. Heinemann, and T. Hoshi. 2004. Reactive oxygen species impair Slo1 BK channel function by altering cysteine-mediated calcium sensing. *Nat. Struct. Mol. Biol.* 11:171–178.

41. Lu, T., T. He, Z. S. Katusic, and H. C. Lee. 2006. Molecular mechanisms mediating inhibition of human large conductance Ca^{2+}-activated K^+ channels by high glucose. *Circ. Res.* 99:607–616.

42. Lu, T., D. Ye, X. Wang, J. M. Seubert, J. P. Graves, J. A. Bradbury, D. C. Zeldin, and H. C. Lee. 2006. Cardiac and vascular KATP channels in rats are activated by endogenous epoxyeicosatrienoic acids through different mechanisms. *J. Physiol. (Lond.)* 575:627–644.

43. Lu, T., P. V. Katakam, M. VanRollins, N. L. Weintraub, A. A. Spector, and H. C. Lee. 2001. Dihydroxyeicosatrienoic acids are potent activators of Ca(2+)-activated K(+) channels in isolated rat coronary arterial myocytes. *J. Physiol. (Lond.)* 534:651–667.

44. Colquhoun, D., and F. J. Sigworth. 1995. Fitting and statistical analysis of single channel recording. *In* Single-Channel Recording, 2nd ed. B. Sakmann, and E. Neher, editors. Plenum Press, New York. 483–587.

45. Qin, F., A. Auerbach, and F. Sachs. 1996. Estimating single-channel kinetic parameters from idealized patch-clamp data containing missed events. *Biophys. J.* 70:264–280.

46. Qin, F., A. Auerbach, and F. Sachs. 2000. Hidden Markov modeling for single channel kinetics with filtering and correlated noise. *Biophys. J.* 79:1928–1944.

47. Bolton, T. B. 2006. Calcium events in smooth muscles and their interstitial cells: physiological roles of sparks. *J. Physiol. (Lond.)* 570: 5–11.

48. Perez, G. J., A. D. Bonev, and M. T. Nelson. 2001. Micromolar Ca^{2+} from sparks activates Ca^{2+}-sensitive K^+ channels in rat cerebral artery smooth muscle. *Am. J. Physiol. Cell Physiol.* 281:C1769–C1775.

49. Magleby, K. L. 2003. Gating mechanism of BK (Slo1) channels: so near, yet so far. *J. Gen. Physiol.* 121:81–96.

50. McManus, O. B., and K. L. Magleby. 1991. Accounting for the Ca(2+)-dependent kinetics of single large-conductance Ca^{2+} -activated K^+ channels in rat skeletal muscle. *J. Physiol. (Lond.)* 443:739–777.

51. Popescu, G., and A. Auerbach. 2003. Modal gating of NMDA receptors and the shape of their synaptic response. *Nat. Neurosci.* 6:476–483.

52. McManus, O. B., G. H. Harris, K. M. Giangiacomo, P. Feigenbaum, J. P. Reuben, M. E. Addy, J. F. Burka, G. J. Kaczorowski, and M. L. Garcia. 1993. An activator of calcium-dependent potassium channels isolated from a medicinal herb. *Biochemistry.* 32:6128–6133.

53. Ferguson, W. B., O. B. McManus, and K. L. Magleby. 1993. Opening and closing transitions for BK channels often occur in two steps via sojourns through a brief lifetime subconductance state. *Biophys. J.* 65: 702–714.

54. Niu, X., and K. L. Magleby. 2002. Stepwise contribution of each subunit to the cooperative activation of BK channels by Ca^{2+}. *Proc. Natl. Acad. Sci. USA.* 99:11441–11446.

55. Moss, G. W., and E. Moczydlowski. 1996. Rectifying conductance substates in a large conductance Ca^{2+} -activated K^+ channel: evidence for a fluctuating barrier mechanism. *J. Gen. Physiol.* 107:47–68.

56. Moss, B. L., S. D. Silberberg, C. M. Nimigean, and K. L. Magleby. 1999. Ca^{2+}-dependent gating mechanisms for dSlo, a large-conductance Ca^{2+}-activated K^+ (BK) channel. *Biophys. J.* 76:3099–3117.

57. Qian, X., X. Niu, and K. L. Magleby. 2006. Intra- and intersubunit cooperativity in activation of BK channels by Ca^{2+}. *J. Gen. Physiol.* 128:389–404.

58. Lauger, P. 1995. Conformational transitions of ionic channels. *In* Single-Channel Recording, 2nd ed. B. Sakmann and E. Neher, editors. Plenum Press, New York. 651–662.

59. Zheng, J., and F. J. Sigworth. 1997. Selectivity changes during activation of mutant *Shaker* potassium channels. *J. Gen. Physiol.* 110:101–117.

60. Zheng, J., and F. J. Sigworth. 1998. Intermediate conductances during deactivation of heteromultimeric *Shaker* potassium channels. *J. Gen. Physiol.* 112:457–474.

61. Tao, T., J. Xie, M. L. Drumm, J. Zhao, P. B. Davis, and J. Ma. 1996. Slow conversions among subconductance states of cystic fibrosis transmembrane conductance regulator chloride channel. *Biophys. J.* 70:743–753.

62. Harrington, M. A., and R. R. Kopito. 2002. Cysteine residues in the nucleotide binding domains regulate the conductance state of CFTR channels. *Biophys. J.* 82:1278–1292.

63. Favre, I., and E. Moczydlowski. 1999. Simultaneous binding of basic peptides at intracellular sites on a large conductance Ca^{2+}-activated K^+ channel. Equilibrium and kinetic basis of negatively coupled ligand interactions. *J. Gen. Physiol.* 113:295–320.

64. Chapman, M. L., and A. M. VanDongen. 2005. K channel subconductance levels result from heteromeric pore conformations. *J. Gen. Physiol.* 126:87–103.